International Journal of Nanoelectronics and Materials
IJNeaM
ISSN 1985-5761 | E-ISSN 2232-1535

Optimizing nanocrystalline cellulose extraction from cigarette filters via sulfuric acid hydrolysis using Box-Behnken design

Menaga Thmil Selvan [a,b], Akmal Hadi Ma'Radzi [a,b] *, Boon-Beng Lee [a,b], Ku Azizah Ku Daud [c], Mohd Faizun Zainol Abidin [c], Sohaizam Ismail [c], Nurul Izwani Abdul Hamid [c], Yusrizal Yusof [c], and Kotchaphan Kanjana [d]

[a]*Faculty of Chemical Engineering & Technology, Universiti Malaysia Perlis (UniMAP), 02600 Arau, Perlis, Malaysia*
[b]*Centre of Excellence for Biomass Utilization, Universiti Malaysia Perlis (UniMAP), 02600 Arau, Perlis, Malaysia*
[c]*Jabatan Kastam Diraja Malaysia, Kompleks Kastam Negeri, Jalan Kampong Pondok, 01000 Kangar, Perlis, Malaysia*
[d]*Department of Chemistry, School of Science, Walailak University, Tha Sala, Nakhon Si Thammarat, 80160, Thailand*
** Corresponding author. Tel.: +60-4-979-8849; e-mail: akmalhadi@unimap.edu.my*

Received 12 September 2025, Revised 1 October 2025, Accepted 10 October 2025

ABSTRACT

The increase in cigarette confiscation by the Royal Malaysian Customs Department led to cigarette burning, contributing to raw materials wastage. Cellulose-rich cigarette filters (CF) can yield nanocrystalline cellulose (NCC) with potential applications in advanced materials. The NCC can be obtained by using sulfuric acid in the acid hydrolysis process. While sulfuric acid hydrolysis is a widely used method for extracting NCC, there is a lack of optimization of its parameters tailored to the cigarette filter as the raw material. This gap hinders the ability to consistently produce high-yield NCC, especially from non-traditional cellulose sources like cigarette butts. This study focuses on optimizing the extraction of NCC via sulfuric acid hydrolysis, utilizing a Box-Behnken experimental design to determine the optimized process parameters. The effects of acid concentration (33–35%), reaction temperature (45–75°C), and hydrolysis time (40–90 min) on NCC yield percentage were evaluated. The FTIR confirmed the removal of non-cellulosic components from the CF without affecting the functional groups of cellulose, confirming that its structural integrity remains unaltered. Findings from this study recorded the highest yield by using sulfuric acid hydrolysis, which can reach up to 89.95% from the cigarette filters used. The findings provide a sustainable approach to turning zero-waste cigarettes' raw materials into sustainable advanced materials.

Keywords: *Nanocrystalline cellulose, Cigarette filter, Sulfuric acid hydrolysis, Box-Behnken design, Optimization*

1. INTRODUCTION

The Royal Malaysian Customs Department conducts raids to seize any possession and trading of illegal tobacco [1]. Illicit tobacco activities lead to the deterioration of public health, as well as causing revenue loss for the government [1, 2]. However, the increasing number of confiscated cigarettes causes inadequate storage space, encouraging the authorities to burn the confiscated cigarettes to prevent them from re-entering the market. Burning cigarettes will contribute to global greenhouse gas emissions and waste of raw materials [2]. Repurposing cigarettes can reduce environmental impacts while giving them an alternative application [3].

Cigarette filters (CF) are made of cellulose acetate, the resultant product from the esterification of natural cellulose with acetic acid [4]. It has minimal lignin and hemicellulose compared to the agricultural biomass. The cellulose acetate requires a deacetylation process to remove the acetyl group, while other biomass will require pre-treatments to remove the lignin and hemicellulose [5, 6]. Unlike common biomass feedstock, cigarette filters have poor biodegradability compared to other cellulosic materials [7]. The presence of acetyl groups hinders microbial degradation and requires specific conditions, such as UV irradiation or the incorporation of titanium dioxide to facilitate photodegradation [7–9]. The common biomass feedstocks have higher biodegradability and lower environmental impact compared to cellulose acetate [7].

Deacetylation of cellulose acetate can be conducted by using sodium hydroxide [3, 10]. Hydrolysis can break the cellulose to produce nanocrystalline cellulose (NCC) [11]. NCC has good mechanical strength, biocompatibility, and sustainable properties. NCCs are widely used in various applications, such as food packaging and medical and water treatment systems [12–14]. Efficient extraction of NCC from the CF is essential to obtain a quality NCC with a high yield and a well-defined nanostructure [15]. The NCC from cigarette filters recorded up to 96.77% crystallinity, while NCC extracted from corncob, pine wood, and sugarcane bagasse recorded 79.3%, 70.9%, and 69.9%, respectively [10, 16, 17]. The average diameter of spherical-shaped NCC from pepper (*Piper nigrum* L.) stalk waste was in the range of 33–67 nm, while the organic acid hydrolysed rod-like NCC has a length of 210–321 nm [18]. The NCC produced from discarded CF has a mean width of 8.3 nm [10].

Sulfuric acid was selected for this study due to its effectiveness in breaking down amorphous regions of cellulose and providing good colloidal stability. Despite its

potential, the process parameters for extracting NCC from CF remain underexplored and insufficiently optimized.

Box-Behnken design is a highly efficient response surface methodology as it requires fewer experimental runs compared to the full factorial design while having reliable experimental results [19, 20]. The suitability of BBD in nanomaterial optimization has been demonstrated in previous studies, where similar designs successfully identified optimal dissolution efficiency and preparation of nanoparticles [21, 22].

Limited research employed the Box-Behnken design to both optimize the yield of NCC and represent the influence of variables through contour plot visualization. The main objective of this study is to find the optimal parameter for NCC extraction with high yield. Box-Behnken design is used as a statistical tool to develop contour plots and to evaluate the parameters' interaction effects. Repurposing the CF contributes to a sustainable path, reducing environmental concerns while producing a valuable nanomaterial.

2. MATERIALS AND METHODS

2.1. Materials

Confiscated cigarettes provided by the Royal Malaysian Customs Department, Perlis. Ethanol, sodium hydroxide (NaOH), and sodium chlorite ($NaClO_2$) were purchased from Chemiz Sdn. Bhd. HmbG Chemicals supplied sulfuric acid (H_2SO_4, 98% purity).

2.2. Pre-treatment of Cigarette Filters

The CF were separated from the confiscated cigarettes and cut into approximately 1 cm in size. The CF then undergoes deacetylation by using 1 M of sodium hydroxide under continuous stirring at room temperature for 1 hour, repeated three times. Then, the CF was bleached at room temperature for 6 hours under constant stirring using 0.2 M sodium chlorite. After each treatment cycle, the CF was thoroughly washed with distilled water to ensure complete residual removal. The treated CF were oven-dried at 50°C for 3 hours before the acid hydrolysis.

2.3. Acid Hydrolysis

Varying concentrations of sulfuric acid were prepared, ranging from 33 to 35%. The concentration of sulfuric acid plays a crucial role in the yield, where previous studies suggest that concentrations around 33% to 37.5% are effective [23, 24]. The optimum hydrolysis time, which is in the range of 40 to 90 minutes, is significant to ensure complete hydrolysis [23, 25]. The hydrolysis temperature was selected according to the literature, with a range from 45 to 75°C [26, 27]. The pre-treated CF undergoes acid hydrolysis with different concentrations (33 to 35%), reaction temperatures (45 to 75°C), and reaction times (40 to 90 minutes) with continuous stirring. After hydrolysis, the reaction was terminated by adding tenfold of distilled water into the mixture. The transparent top layer of the mixture was discarded. Then, the mixture was centrifuged at 3,500 rpm for 10 minutes (Compact Tabletop Refrigerated Centrifuge, Kubota 2800, Japan). The turbid supernatant was collected for further centrifugation at 3,500 rpm for 45 minutes to achieve a neutral pH. The solution was then oven-dried at 50°C overnight.

2.4. Fourier Transform Infrared Spectroscopy (FTIR)

The Fourier Transform Infrared Spectroscopy (Perkin Elmer Spectrum-65, USA) was used to determine the chemical structure of the resultant NCC compared with treated CF. FTIR acquired by 32 scans of the sample with the wavelength range of 4000 cm^{-1} to 400 cm^{-1} with the KBr pellet method.

2.5. Particle Size Analyser and Zeta Potential

Dynamic light scattering (DLS) (Malvern Zetasizer Lab, UK) was used to measure the NCC suspension's particle size and zeta potential. The reflected laser light of DLS by NCC particles produces frequency shifts to determine particle size. The suspension was sonicated for 5–10 minutes to ensure proper dispersion. The NCC particle measurement range was set from 0.1 nm to 10 µm, and the measurement angle was set to 90°. Measurements were conducted at 25°C using disposable capillary cells. Zeta potential assessed the nanocellulose particles' surface charge and colloidal stability. The sample was prepared in a 2 mL volume.

2.6. Experimental Design (Box-Behnken)

A Box-Behnken Design (BBD) was chosen to study the effects of acid concentration, reaction temperature, and reaction time, with each factor at three levels using Minitab statistical software (Minitab Inc., USA). The interaction between factors was investigated with a minimal number of experimental runs. The three variables were varied, where acid concentrations (33–35%), reaction temperature (45–75°C), and reaction time (40–90 minutes). The response variable is the percentage of yield of NCC (%). The BBD generated 15 experimental runs, providing a systematic framework as shown in Table 1. The

Table 1. Box-Behnken experimental design

Run	Concentration (%)	Temperature (°C)	Time (minute)
1	33	45	60
2	33	75	60
3	33	60	40
4	33	60	90
5	34	45	40
6	34	75	40
7	34	45	90
8	34	75	90
9	34	60	60
10	34	60	60
11	34	60	60
12	35	45	60
13	35	75	60
14	35	60	40
15	35	60	90

experimental data obtained from the runs were used to develop a regression equation to investigate the relationship between each variable and the NCC yield (%). The statistical significance of the model was assessed using Analysis of Variance (ANOVA) and contour plots to identify the interaction of factors on the yield of NCC.

3. RESULTS AND DISCUSSION

3.1. FTIR Analysis

The FTIR graph of treated CF and NCC is shown in Figure 1. The hydroxyl peak is present at 3651 cm^{-1} with different intensities [28]. The intense hydroxyl peak of NCC shows a high hydroxyl group aligning with the cellulose structure. The alkyl peak is observed at 2897 cm^{-1}, which is related to aliphatic chains in cellulose structure, a similar peak found by Reis *et al.* [29]. The alkyl peak is minimal for treated CF compared to NCC because the CF has low cellulose content. The peak at 1641 cm^{-1} belongs to the hydroxyl group attributed to absorbed moisture by the sample as reported by Wulandari *et al.* [30]. The NCC has a high intensity of 1641 cm^{-1} peak exhibiting a hydrophilic property [31]. The crystalline cellulose peak of NCC has a higher peak at 1376 cm^{-1} than CF, indicating more crystalline structures similar to Hamed *et al.* [32]. Peaks at 996 cm^{-1} and 893 cm^{-1} belong to C–O stretching and β-glycosidic linkage, indicating the presence of cellulose structure [33]. The CF has a weak peak at both carbonyl and β-glycosidic linkage due to a less defined cellulose structure. The expected peak of the lignin at 1606 cm^{-1} is not present, suggesting complete lignin removal. The hemicellulose peak at 1426 cm^{-1} also disappeared due to pretreatments involved in removing both hemicellulose and lignin. The FTIR result proves the successful NCC extraction by acid hydrolysis.

3.2. Particle Size Analyser and Zeta Potential

The nanocellulose suspension's particle size distribution and zeta potential were analyzed using Dynamic Light Scattering (DLS). The particle size of NCC obtained with parameters of 34%, 60°C, and 60 minutes (NCC60), and 34%, 75°C, and 90 minutes (NCC75), was within the nanometer range, confirming its nanoscale dimensions and uniformity. The analysis showed that the NCC60 exhibited a dominant particle size of 15.7 nm with an intensity of 90.9%. Different particle sizes of 13.5 nm and 18.2 nm were present as well, but with intensities of 3.37% and 5.73%, respectively. The range of particle sizes detected suggests that the NCC suspension has a narrow particle size and monodisperse distribution. In a study by Ilyas *et al.* [25], the NCC from sugar palm fiber sizes differ according to the hydrolysis time, from 7.5 nm to 13 nm, supporting the relevance of the result obtained for NCC60. The NCC75 has a broad distribution of particle size ranging from 396 nm to 615 nm. The highest intensity is present in 531 nm and 459 nm with intensities of 45.1% and 42.4%, respectively. In contrast, a study by Wulandari *et al.* [30] found that the maximum particle size of NCC from sugarcane bagasse was 148.4 nm. The particle size of NCC75 explains the Van der Waals force between the particles to form aggregation [34]. Nanoparticles in aqueous media tend to undergo aggregation due to interfacial interactions and transport dynamics, forming micro-sized clusters, affecting the particle size analysis [35].

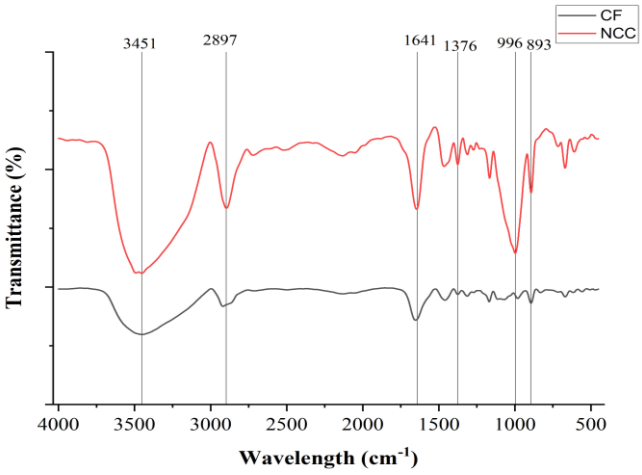

Figure 1. FTIR graph of treated CF and NCC

The Zetasizer recorded a zeta potential value of –29.4 mV and –22.3 mV, indicating good colloidal stability for NCC60 and NCC75, respectively. The presence of sufficient repulsive force between particles prevents aggregation. The negative charge of NCC is attributed to the esterification process by the sulfate ions' hydroxyl group, resulting in a stable colloid system [11]. Zeta potential with more than –15 mV indicates suspension stability, while a value greater than –30 mV exhibits colloidal stability [15]. These findings confirm that the sample preparation was effective, leading to well-dispersed, stable nanoparticles suitable for further functionalization or incorporation into polymer matrices.

3.3. Comparison of Predicted and Experimental NCC Yield

The NCC yield was predicted using the regression model generated by Minitab's analysis. These predicted values are compared with the actual experimental yields, as shown in Table 2. The predicted value of NCC yield is approximately close to the actual NCC yield, especially in mid-range and high-yield conditions. The highest yield at the parameter, 34% acid concentration, 75°C temperature, and 90 minutes reaction time, a minimal deviation of 2.21% occurs between the predicted and actual value. However, some differences occur, especially under extreme conditions such as at 35% acid concentration, 45°C, and 60 minutes, where the model predicted a negative yield of –8.50%, while the actual yield was 0.45%.

3.4. Model Fitting and ANOVA

The regression equation of the model shown in Equation (1) shows that the most significant linear factor influencing NCC yield is acid concentration. The increase in acid concentration will increase the NCC yield, as indicated by the positive coefficient. The high sulfuric acid concentration will enhance the breakdown of amorphous regions in the CF. The hydrolysis temperature has a slightly

Table 2. The predicted and actual value of NCC yield

Acid Concentration (%)	Temperature (°C)	Time (minutes)	Actual yield (%)	Predicted yield (%)
33	45	60	1.75	1.38
33	75	60	29.65	38.60
33	60	40	15.75	12.13
33	60	90	41.40	36.45
34	45	40	13.69	17.76
34	75	40	48.00	40.88
34	45	90	1.30	6.55
34	75	90	89.95	87.74
34	60	60	65.10	64.97
34	60	60	64.80	64.97
34	60	60	65.00	64.97
35	45	60	0.45	–8.50
35	75	60	46.60	46.97
35	60	40	9.90	16.57
35	60	90	26.00	27.91

$$\begin{aligned}\text{Yield} = {} & -34746 + 2040(\text{Concentration}) - 3.02(\text{Temperature}) + 5.33(\text{Time}) \\ & - 30.16(\text{Concentration} \times \text{Concentration}) - 0.0675(\text{Temperature} \times \text{Temperature}) \\ & - 0.02221(\text{Time} \times \text{Time}) + 0.304(\text{Concentration} \times \text{Temperature}) - 0.130(\text{Concentration} \times \text{Time}) \\ & + 0.0387(\text{Temperature} \times \text{Time}) \end{aligned} \quad (1)$$

antagonistic effect on the NCC yield, where high temperatures may lead to the potential degradation of NCC's structural integrity and crystallinity, decreasing its yield.

In a study by Yu *et al.* [36], the increase in temperature decreased the NCC yield significantly from 94.8% to 90.5%. The hydrolysis time has a synergistic effect on the NCC yield. A prolonged reaction time increases the NCC yield. Contrary to a study by Ilyas *et al.* [25], the increase of reaction time from 30 minutes to 60 minutes lowers the yield from 33.51% to 13.12%. However, the quadratic effect of acid concentration, reaction temperature, and reaction time has an antagonistic impact on the NCC yield in cases of too high acid concentration, very high temperature, and extended reaction time. These conditions will lead to degrading the NCC and lowering its yield, suggesting an optimal range for each factor. A synergistic effect is observed in the interaction between acid concentration and temperature and between temperature and time. A balanced combination of process parameters can promote the NCC yield. In contrast, the interaction effect of concentration and reaction time has a negative impact on the NCC yield.

The statistical significance of the regression model was evaluated by Analysis of Variance (ANOVA) to determine the influence of reaction parameters on NCC yield, as shown in Table 3. The F-value of the model is 17.19, with a p-value of 0.003, indicating that the regression model is statistically significant. The hydrolysis temperature factor has a high significance on NCC yield, followed by reaction time and acid concentration. The relationship between acid concentration and NCC yield is not linear. The quadratic effect of acid concentration is highly significant, with a p-value of 0.001. The quadratic effect suggests that the response responds in a non-linear producing an optimal level of acid concentration. Pandi *et al.* [37] reported that higher acid concentrations adversely affected the quality of the NCC produced, highlighting the significant influence of acid concentration on NCC yield. All three factors are significant, with a p-value lower than 0.05 implying that each parameter's highest or lowest point may influence the NCC yield negatively. The effects of temperature and time interaction were the only significant ones on NCC yield. The reaction temperature and time balance can significantly enhance the NCC yield. A significant lack of fit is detected in the model due to outliers, where the model overpredicted or underpredicted the yield.

The standard error of the estimate (S) is 8.31878, representing the observed value tolerance compared to the regression line. The low value of S indicates that the actual value is close to the predicted value, which indicates a good model fit. The model explains 96.87% variations in NCC yield according to the R-squared value. The adjusted R-squared 91.24% value indicates a good model significance with a good fit between theoretical and experimental. The predicted R-squared measures show that the model is able to generalize 50.15% of new data.

Table 3. Analysis of variance (ANOVA) of NCC yield based on Box-Behnken design

Source	DF	Adj SS	Adj MS	F-Value	P-Value
Model	9	10709.2	1189.91	17.19	0.003
Linear	3	5979.7	1993.25	28.80	0.001
Concentration	1	8.2	8.24	0.12	0.744
Temperature	1	5335.9	5335.87	77.11	0.000
Time	1	635.6	635.64	9.19	0.029
Square	3	4347.3	1449.10	20.94	0.003
Concentration*Concentration	1	3359.4	3359.36	48.54	0.001
Temperature*Temperature	1	852.0	852.04	12.31	0.017
Time*Time	1	643.6	643.57	9.30	0.028
2-Way Interaction	3	986.1	328.70	4.75	0.063
Concentration*Temperature	1	83.3	83.27	1.20	0.323
Concentration*Time	1	43.0	42.97	0.62	0.466
Temperature*Time	1	859.9	859.88	12.43	0.017
Error	5	346.0	69.20		
Lack-of-Fit	3	346.0	115.32	4942.34	0.000
Pure Error	2	0.0	0.02		
Total	14	11055.2			

3.5. Contour Plots of Interactions Between Variables on NCC Yield

The contour plot visualizes the effect of two independent variables on the NCC yield. Figure 2 shows that the moderate spacing between the contour lines indicates a gradual change in NCC yield as temperature and acid concentration increase. High acid concentration results in low yield because of NCC degradation to the simplest form, glucose [36, 37]. The weak interaction between concentration and temperature shows that it independently affects hydrolysis. The pattern indicates a progressive effect on the NCC yield and provides controllable improvements. The contour plot shows that the highest yield was obtained at a temperature of more than 57.13°C with an acid concentration of 33.37% to 34.73%. High reaction temperature facilitates the breakdown of the cigarette filter into NCC, removing the amorphous regions [38].

Figure 3 shows the interaction effect of acid concentration and reaction time on NCC yield. The closely spaced contour lines exhibit the steep gradient in NCC yield with a minor acid concentration or reaction time adjustment. The high sensitivity may cause high yield fluctuations even if a slight variation in either factor occurs, providing a narrow process window. A study by Kusmono *et al.* [39] recorded a decrease in NCC crystallite size as the acid concentration and hydrolysis time increased due to dissolution of both amorphous and crystalline regions. A yield of NCC higher than 60% is expected with time above 53.28 minutes and acid concentration in a range of 33.42 to 34.5%. An increase in hydrolysis time produces a high yield of NCC with an optimum acid concentration range [40].

The interaction of reaction time and reaction temperature is shown in Figure 4. The large contour line spacing shows that the NCC yield changes slowly as the reaction time and temperature change. A previous study recorded a minimal change in yield percentage as the reaction temperature and time were adjusted. Yu *et al.* [36] observed a yield variation of 0.8% with a one-hour change in reaction time, and a 1.1% difference associated with a 10°C change in reaction temperature. High NCC yield is encountered at a longer reaction time and high temperature. This condition improves the hydrolysis due to the thermal disruption of the cellulose structure. The interaction has a p-value below 0.05, confirming a significant synergistic effect between reaction time and temperature on NCC yield. The highest NCC yield is observed when the reaction temperature is above 66.55°C and the time is above 73.34 minutes. However, further increase of temperature and time may lead to NCC becoming soluble [39].

4. CONCLUSION

This study successfully optimized the extraction of NCC from CF via sulfuric acid hydrolysis. The effects of acid concentration, reaction temperature, and hydrolysis time on NCC yield were studied using a BBD. The highest experimental NCC yield was achieved at 34% sulfuric acid concentration, 75°C, and 90 minutes, with minimal deviation from the predicted value, indicating strong model accuracy and reliability. The acid concentration showed the most significant positive effect on yield, while hydrolysis temperature had an antagonistic effect on NCC yield. The interaction of acid concentration and temperature is weak, as it has an independent effect on NCC yield. A strong synergistic interaction between temperature and time was

evident from the gradual yield increase observed in contour plots. These findings highlight the importance of optimizing extraction parameters to maximize NCC yield, promoting sustainability and waste valorization.

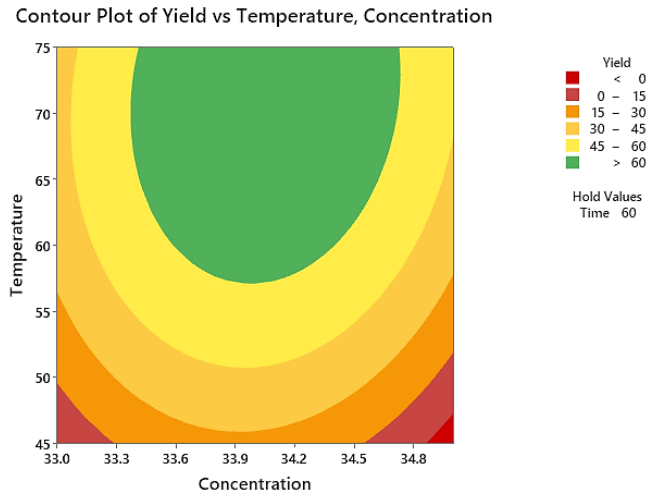

Figure 2. Contour plot of concentration and temperature effects on NCC yield.

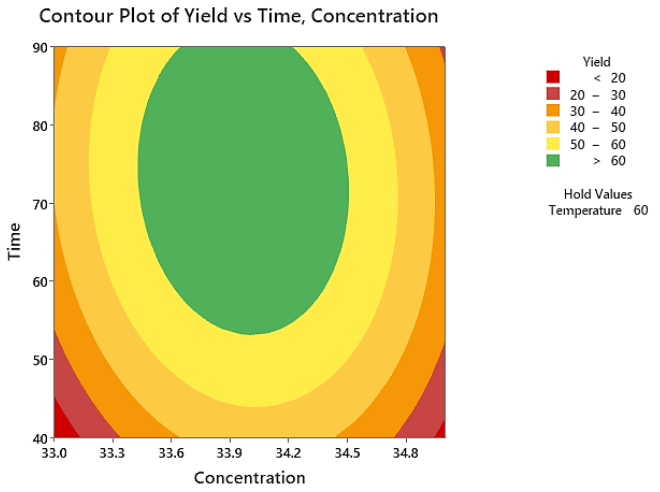

Figure 3. Contour plot of concentration and time effects on NCC yield.

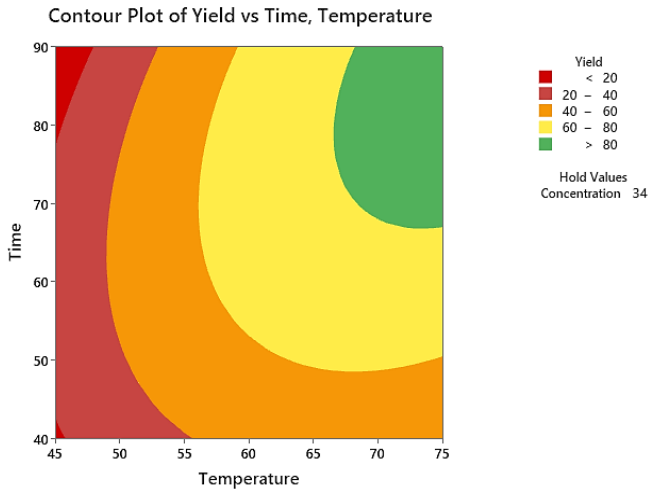

Figure 4. Contour plot of temperature and time effects on NCC yield.

ACKNOWLEDGMENTS

The authors would like to acknowledge the Ministry of Higher Education Malaysia for the financial support under grant reference no: FRGS/1/2023/STG05/UNIMAP/02/3. Appreciations are also extended to the Faculty of Chemical Engineering & Technology, Universiti Malaysia Perlis, for providing support.

REFERENCES

[1] R. K. Koya, J. R. Branston, and A. W. A. Gallagher, "Measuring Malaysia's Illicit Tobacco Trade: An Excise Tax Gap Analysis," *Journal of Illicit Economies and Development*, vol. 4, no. 1, pp. 58–70, 2022.

[2] M. Yousefi, M. Kermani, M. Farzadkia, K. Godini, and J. Torkashvand, "Challenges on the recycling of cigarette butts," Jun. 01, 2021, *Springer Science and Business Media Deutschland GmbH*.

[3] M. H. K. N. M. A. and N. A. Y. Azlan, "Nanocrystalline Cellulose Extracted From Discarded Cigarette Butts," *Malaysian Journal of Analytical Sciences*, vol. 28, pp. 500–511, 2024.

[4] H. Kurmus and A. Mohajerani, "The toxicity and valorization options of cigarette butts," Mar. 01, 2020, *Elsevier Ltd*.

[5] A. Sidana and S. K. Yadav, "Recent developments in lignocellulosic biomass pretreatment with a focus on eco-friendly, non-conventional methods," *Journal of Cleaner Production*, vol. 335, 2022.

[6] N. Tulos, D. Harbottle, A. Hebden, P. Goswami, and R. S. Blackburn, "Kinetic Analysis of Cellulose Acetate/Cellulose II Hybrid Fiber Formation by Alkaline Hydrolysis," *ACS Omega*, vol. 4, no. 3, pp. 4936–4942, 2019.

[7] J. Puls, S. A. Wilson, and D. Hölter, "Degradation of Cellulose Acetate-Based Materials: A Review," *Journal of Polymers and the Environment*, vol. 19, pp. 152–165, 2011.

[8] S. Peil, H. Gojzewski, and F. R. Wurm, "Reversible acetalization of cellulose: A platform for bio-based materials with adjustable properties and biodegradation," *Chemical Engineering Journal*, vol. 452, 2023.

[9] B. Mušič, A. Jemec Kokalj, and A. Sever Škapin, "Influence of Weathering on the Degradation of Cellulose Acetate Microplastics Obtained from Used Cigarette Butts," *Polymers (Basel)*, vol. 15, no. 12, 2023.

[10] S. A. Ogundare, V. Moodley, and W. E. van Zyl, "Nanocrystalline cellulose isolated from discarded cigarette filters," *Carbohydrate Polymers*, vol. 175, pp. 273–281, 2017.

[11] P. Phanthong, P. Reubroycharoen, X. Hao, G. Xu, A. Abudula, and G. Guan, "Nanocellulose: Extraction and application," Apr. 01, 2018, *KeAi Publishing Communications Ltd.*

[12] Abdullah *et al.*, "Biopolymer-based functional films for packaging applications: A review," Aug. 22, 2022, *Frontiers Media S.A.*

[13] M. Leonovich, V. Korzhikov-Vlakh, A. Lavrentieva, I. Pepelanova, E. Korzhikova-Vlakh, and T. Tennikova,

"Poly(lactic acid) and Nanocrystalline Cellulose Methacrylated Particles for Preparation of Cryogelated and 3D-Printed Scaffolds for Tissue Engineering," *Polymers (Basel)*, vol. 15, no. 3, 2023.

[14] P. G. Marakana, A. Dey, and B. Saini, "Isolation of nanocellulose from lignocellulosic biomass: Synthesis, characterization, modification, and potential applications," Dec. 01, 2021, *Elsevier Ltd*.

[15] G. Parsai, P. A. Parikh, and J. K. Parikh, "Novel DES-ultrasonication assisted process for nanocellulose synthesis using Box Behnken design," *Industrial Crops and Products*, vol. 217, 2024.

[16] F. I. Ditzel, E. Prestes, B. M. Carvalho, I. M. Demiate, and L. A. Pinheiro, "Nanocrystalline cellulose extracted from pine wood and corncob," *Carbohydrate Polymers*, vol. 157, pp. 1577–1585, 2017.

[17] S. Mishra, "New Excipient for Oral Drug Delivery: CNC Derived from Sugarcane Bagasse-Derived Microcrystalline Cellulose," *ACS Omega*, vol. 9, no. 17, pp. 19353–19362, 2024.

[18] H. Holilah *et al.*, "Uniform rod and spherical nanocrystalline celluloses from hydrolysis of industrial pepper waste (*Piper nigrum* L.) using organic acid and inorganic acid," *International Journal of Biological Macromolecules*, vol. 204, pp. 593–605, 2022.

[19] S. Beg and S. Akhter, "Box–Behnken Designs and Their Applications in Pharmaceutical Product Development," *Design of Experiments for Pharmaceutical Product Development Volume I: Basics and Fundamental Principles*, vol. 1, pp. 77–85, 2021.

[20] S. Beg and K. Raza, "Full Factorial and Fractional Factorial Design Applications in Pharmaceutical Product Development," *Design of Experiments for Pharmaceutical Product Development Volume I: Basics and Fundamental Principles*, vol. 1, pp. 43–53, 2021.

[21] R. R. Zaky, M. M. Hessien, A. A. El-Midany, M. H. Khedr, E. A. Abdel-Aal, and K. A. El-Barawy, "Preparation of silica nanoparticles from semi-burned rice straw ash," *Powder Technology*, vol. 185, no. 1, pp. 31–35, 2008.

[22] S. Özer-önder and T. Uğurlu, "Application of Box-Behnken design in the optimization of chitosan nanoparticles prepared by the ionic gelation-ultrasonication method and evaluation of dispersion stability," *Journal of Research in Pharmacy*, vol. 28, no. 4, pp. 1057–1068, 2024.

[23] K. Diharjo, F. Gapsari, A. Andoko, R. Septiari, S. M. Rangappa, and S. Siengchin, "Optimization of nano cellulose extraction from timoho fiber using response surface methodology (RSM)," *Biomass Conversion and Biorefinery*, vol. 14, no. 20, pp. 25557–25567, 2024.

[24] P. P. Zou, P. Zhang, D. Gao, and Q. N. Xia, "Process' Optimization of Nanocrystalline Cellulose and its Properties," *Applied Mechanics and Materials*, vol. 200, pp. 373–376, 2012.

[25] R. A. Ilyas *et al.*, "Effect of hydrolysis time on the morphological, physical, chemical, and thermal behavior of sugar palm nanocrystalline cellulose (Arenga pinnata (Wurmb.) Merr)," *Textile Research Journal*, vol. 91, no. 1–2, pp. 152–167, 2021.

[26] S. Dong, M. J. Bortner, and M. Roman, "Analysis of the sulfuric acid hydrolysis of wood pulp for cellulose nanocrystal production: A central composite design study," *Industrial Crops and Product*, vol. 93, pp. 76–87, 2016.

[27] J. Bouchard, M. Méthot, C. Fraschini, and S. Beck, "Effect of oligosaccharide deposition on the surface of cellulose nanocrystals as a function of acid hydrolysis temperature," *Cellulose*, vol. 23, no. 6, pp. 3555–3567, 2016.

[28] H. A. Nabwey, M. Abdelkreem, M. A. Tony, and N. F. Al Hoseny, "Smart win–win waste management: superhydrophobic filter using valorized cellulose acetate from discarded cigarette butts for cleaning up marine oil spill at Hurghada Red Sea shore in Egypt," *Frontiers in Marine Science*, vol. 11, 2024.

[29] R. R. dos Reis, C. Effting, and A. Schackow, "Cellulose nanofibrils on lightweight mortars for improvement of the performance of cement systems," *Carbohydrate Polymer Technologies and Applications*, vol. 5, p. 100303, 2023.

[30] W. T. Wulandari, A. Rochliadi, and I. M. Arcana, "Nanocellulose prepared by acid hydrolysis of isolated cellulose from sugarcane bagasse," in *IOP Conference Series: Materials Science and Engineering*, Institute of Physics Publishing, Feb. 2016.

[31] K. Makhliyo, A. Abdumutolib, S. Sirojiddin, A. Nurbek, Y. Khaydar, and G. Jiang, "Preparation of oxidized nanocellulose by using potassium dichromate," *Cellulose*, vol. 30, no. 9, pp. 5657–5668, 2023.

[32] S. A. A. K. M. Hamed and M. L. Hassan, "A new mixture of hydroxypropyl cellulose and nanocellulose for wood consolidation," *Journal of Cultural Heritage*, vol. 35, pp. 140–144, 2019.

[33] M. Babicka *et al.*, "Nanocellulose Production Using Ionic Liquids with Enzymatic Pretreatment," *Materials*, vol. 14, no. 12, p. 3264, 2021.

[34] S. Shrestha, B. Wang, and P. Dutta, "Nanoparticle processing: Understanding and controlling aggregation," *Advances in Colloid and Interface Science*, vol. 279, p. 102162, 2020.

[35] W. Zhang, "Nanoparticle Aggregation: Principles and Modeling," in *Advances in Experimental Medicine and Biology*, 2014, pp. 19–43.

[36] H. Yu, Z. Qin, B. Liang, N. Liu, Z. Zhou, and L. Chen, "Facile extraction of thermally stable cellulose nanocrystals with a high yield of 93% through hydrochloric acid hydrolysis under hydrothermal conditions," *Journal of Materials Chemistry A*, vol. 1, no. 12, p. 3938, 2013.

[37] N. Pandi, S. H. Sonawane, and K. Anand Kishore, "Synthesis of cellulose nanocrystals (CNCs) from cotton using ultrasound-assisted acid hydrolysis," *Ultrasonics Sonochemistry*, vol. 70, 2021.

[38] L. Chen, Q. Wang, K. Hirth, C. Baez, U. P. Agarwal, and J. Y. Zhu, "Tailoring the yield and characteristics of wood cellulose nanocrystals (CNC) using concentrated acid hydrolysis," *Cellulose*, vol. 22, no. 3, pp. 1753–1762, 2015.

[39] Kusmono and M. N. Affan, "Isolation and Characterization of Nanocrystalline Cellulose from Ramie Fibers via Phosphoric Acid Hydrolysis," *Journal of Natural Fibers*, vol. 19, no. 7, pp. 2744–2755, 2022.

[40] Z. Li *et al.*, "Bleaching-free, lignin-tolerant, high-yield production of nanocrystalline cellulose from lignocellulosic biomass," *iScience*, vol. 26, no. 1, p. 105771, 2023.